Crystal Structures of Human DNA Polymerase β Complexed with Gapped and Nicked DNA: Evidence for an Induced Fit Mechanism[†,‡]

Michael R. Sawaya,[*,§] Rajendra Prasad,[∥] Samuel H. Wilson,[∥] Joseph Kraut,[§] and Huguette Pelletier[⊥]

Department of Chemistry and Biochemistry, University of California, San Diego, 9500 Gilman Drive, La Jolla, California 92093-0506, National Institute of Environmental Health Sciences, P.O. Box 12233, Research Triangle Park, North Carolina 27709-2233, and Verna and Marrs McLean Department of Biochemistry, Baylor College of Medicine, One Baylor Plaza, Houston, Texas 77030

Received February 19, 1997[⊗]

ABSTRACT: DNA polymerase β (pol β) fills single nucleotide (nt) gaps in DNA produced by the base excision repair pathway of mammalian cells. Crystal structures have been determined representing intermediates in the 1 nt gap-filling reaction of pol β: the binary complex with a gapped DNA substrate (2.4 Å resolution), the ternary complex including ddCTP (2.2 Å), and the binary product complex containing only nicked DNA (2.6 Å). Upon binding ddCTP to the binary gap complex, the thumb subdomain rotates into the closed conformation to contact the otherwise solvent-exposed ddCTP-template base pair. Thumb movement triggers further conformational changes which poise catalytic residue Asp192, dNTP, and template for nucleotidyl transfer, effectively assembling the active site. In the product nicked DNA complex, the thumb returns to the open conformation as in the gapped binary DNA complex, facilitating dissociation of the product. These findings suggest that pol β may enhance fidelity by an induced fit mechanism in which correct base pairing between template and incoming dNTP induces alignment of catalytic groups for catalysis (via thumb closure), but incorrect base pairing will not. The structures also reveal that pol β binds both gapped and nicked DNA with a 90° kink occurring precisely at the 5′-phosphodiester linkage of the templating residue. If the DNA were not kinked in this way, contact between the thumb and dNTP-template base pair, presumably important for the checking mechanism, would be impossible, especially when the gap is but a single nucleotide. Such a 90° kink may be a mechanistic feature employed by any polymerase involved in filling gaps to completion.

It is a startling fact of life that the DNA in every cell of the human body is spontaneously damaged more than 10 000 times every day (Lindahl, 1993). The base excision repair (BER)[1] pathway is the primary repair system used by the cell to maintain genome integrity under endogenous conditions in which hydrolysis, reactive oxygen species, and other intracellular metabolites modify DNA bases (Seeberg et al., 1995). In this pathway, the damaged base of a nucleotide residue is hydrolyzed by a DNA glycosylase, the backbone is incised by an AP-endonuclease or AP-lyase, and the remaining deoxyribose phosphate residue is excised by a phosphodiesterase or lyase. A DNA polymerase then fills in the single nucleotide gap with the dNTP complementary to the template, and finally the nicked phosphodiester backbone is reconnected by DNA ligase.

In mammalian cells, the penultimate step, gap filling, is performed by DNA polymerase β (Sobol et al., 1996), the smallest of the four nuclear DNA polymerases. Its small size (39 kDa) and lack of intrinsic exonuclease activity make pol β a simple and convenient target for mechanistic studies of template-directed nucleotidyl transfer, i.e., the polymerase reaction. Pol β is composed of only two domains, an N-terminal 8-kDa domain which exhibits deoxyribosephosphate lyase activity (Matsumoto & Kim, 1995) and a C-terminal 31-kDa domain which possesses nucleotidyl transfer activity (Kumar et al., 1990). The 31-kDa domain, like all other structurally characterized polymerases to date, contains fingers, palm, and thumb subdomains, with similarly positioned conserved catalytic residues (Davies et al., 1994; Sawaya et al., 1994). Thus, in many ways pol β may well serve as a model for other more complex polymerases.

Probably the foremost mystery about the BER gap-filling reaction, or indeed any other template-directed nucleotidyl transfer, is the mechanism by which the polymerase enhances fidelity. Here "fidelity" refers to the accuracy of a polymerase in selecting from a pool of four (dATP, dCTP, dGTP, dTTP) the single dNTP that is complementary to the template residue. For example, although one of the least accurate polymerases known, pol β fills short gaps in DNA with a base substitution error frequency up to 200-fold better than the discrimination that would be provided by free energy differences between correct and incorrect pairing in solution (Beard et al., 1996) (see detailed discussion below). Since the original discovery of pol I, numerous mechanisms have been proposed to explain how these energy differences are enhanced in the polymerase active site [for reviews, see

[†] Supported by NIH Grant GM52860 and USPHS Training Grants DK07233 and HG00005.

[‡] Coordinates and reflection data are available from the Brookhaven Protein Data Bank. See Table 1 for PDB entry codes.

* To whom correspondence should be addressed. Email: mrs@heckle.med.harvard.edu.

[§] University of California, San Diego.

[∥] National Institute of Environmental Health Sciences.

[⊥] Baylor College of Medicine.

[⊗] Abstract published in *Advance ACS Abstracts,* September 1, 1997.

[1] Abbreviations: AP, apurinic/apyrimidinic; BER, base excision repair; dNTP, 2′-deoxyribonucleoside 5′-triphosphate; ddNTP, 2′,3′-dideoxyribonucleoside 5′-triphosphate; HhH, helix−hairpin−helix; nt, nucleotide; pol β, DNA polymerase β.

S0006-2960(97)00381-4 CCC: $14.00

Beckman and Loeb (1993), Echols and Goodman (1991), and Johnson (1993)]. Induced fit, initially proposed to explain enzyme specificity in the protein synthesis pathway (Koshland, 1958), was one of the first models proposed to explain polymerase fidelity (Kornberg, 1969; Freese & Freese, 1967) and is still one of the best supported mechanisms today (Wong et al., 1991). Simply put, the induced fit model states that conformational changes induced by binding the correct substrate will bring the catalytic groups into proper alignment for catalysis, whereas the incorrect substrate will not.

Structural evidence suggests that the induced fit model may enhance fidelity in pol β. Prominent movement of the entire thumb subdomain (up to 7 Å for main chain atoms) is evident from comparisons among previously determined pol β structures: the rat apoenzyme (Sawaya et al., 1994), the rat pol β·template-primer·ddCTP ternary complex (Pelletier et al., 1994), and human pol β·template-primer complexes (Pelletier et al., 1996a,b; Beard et al., 1996). According to our previous proposals (Pelletier et al., 1996a,b), the thumb conformation induced by correct dNTP-template base pairing could bring active site residues into alignment for nucleotidyl transfer, whereas the thumb conformation favored by a mismatch may not. Though an induced fit mechanism seems plausible, structural evidence has been incomplete; none of the solved structures has yet revealed the conformation of a gapped DNA substrate (the biologically relevant substrate) in the active site nor has the possible role of crystal packing been addressed in accounting for observed conformational changes.

To investigate the role of DNA conformation and enzyme motion in enhancing fidelity in the BER gap filling reaction, human pol β was crystallized in complexes representing three intermediates of the reaction: the binary complex with a DNA substrate containing a 1 nt gap, the ternary complex including ddCTP, and the product complex containing only nicked DNA.[2] All three complexes crystallized under similar crystal packing conditions in a new crystal form (space group $P2_1$), so conformational distortions caused by packing artifacts should be minimal. From comparisons among these structures, we identify conformational changes and infer when they occur in the reaction cycle. The structures offer new details in support of an induced fit mechanism and suggest the role of an observed 90° kink in the gapped DNA substrate in enhancing fidelity of the polymerase reaction. Additionally, the higher resolution of the human ternary complex (2.2 Å) offers further insights into the nucleotidyl transfer mechanism.

EXPERIMENTAL PROCEDURES

Preparation of Pol β·DNA Complexes. Recombinant human DNA pol β was overexpressed in *Escherichia coli* and purified as described (Abbotts et al., 1988). Pol β was concentrated and stored as described in Pelletier et al. (1996a). DNA oligonucleotides were purchased from Integrated DNA Technologies, Inc. (Coralville, IA). The particular DNA sequence was designed to minimize the chance of slippage between complementary strands. Template, primer, and downstream oligo in a 1:1:1 molar ratio were dissolved and mixed in 20 mM $MgCl_2$, 0.1 M Tris pH 7.5, 25 °C, to a final concentration of 2 mM gapped/nicked DNA. Pol β·DNA complexes were prepared by mixing 480 μL of 20 mg/mL pol β with 240 μL of DNA solution at 4 °C.

Crystallization of Pol β·Gap. Binary pol β·gap crystals were prepared by mixing 5 μL of pol β·gap with 5 μL of a reservoir solution containing 13.8% PEG 3350, 360 mM sodium acetate, and 50 mM imidazole, pH 7.0. DNA sequences corresponding to the template, primer, and downstream oligonucleotide of the gap are 5′-CCGACGGCG-CATCAGC-3′, 5′-GCTGATGCGC-3′, and 5′-pGTCGG-3′. The downstream oligo was 5′-phosphorylated. When properly annealed, these strands form double-stranded DNA with a gap of 1 nt. Crystals were macroseeded once to achieve diffractable size, which usually required 4−5 days at room temperature.

Crystallization of Pol β·Gap·ddCTP. Ternary pol β·gap·ddCTP complex was prepared by adding solid ddCTP to pol β·gap in an 8-fold molar excess at 4 °C. DNA sequences corresponding to the template, primer, and downstream oligonucleotide of the gap are 5′-CCGACGGCG-CATCAGC-3′, 5′-GCTGATGCG-3′, and 5′-pGTCGG-3′. The downstream oligo was 5′-phosphorylated. When properly annealed, these strands form double-stranded DNA with a gap of 2 nt. As anticipated from previous crystallizations with rat pol β ternary complex (Pelletier et al., 1994), human pol β transferred ddCTP onto the 3′ terminus of the primer, extending it by one nucleotide with the final result of a single-nucleotide gap. Pol β cannot extend the dideoxy-terminated primer any further so another ddCTP molecule can then take its position in the dNTP binding site to produce a Michaelis complex analogue. Crystals were prepared by mixing 5 μL of pol β·gap·ddCTP with 5 μL of a reservoir solution containing 16.0% PEG 3350, 180 mM sodium acetate, and 50 mM HEPES, pH 7.5. Crystals were streak-seeded, requiring only 2−3 days to reach maximum size at room temperature.

Crystallization of Pol β·Nick. Pol β·nick crystals were prepared by mixing 5 μL of pol β·nick with 5 μL of a reservoir solution containing 17.5% PEG 3350, 90 mM sodium acetate, and 50 mM imidazole, pH 7.0. DNA sequences corresponding to the template, primer, and downstream oligonucleotide of the gap are 5′-CCGACCACG-CATCAGC-3′, 5′-GCTGATGCGTG-3′, and 5′-pGTCGG-3′. The downstream oligo was 5′-phosphorylated. When properly annealed, these strands form double-stranded DNA containing a nick in the phosphodiester backbone. Crystals were macroseeded once to achieve diffractable size, which usually required 4−5 days at room temperature.

Data Collection and Structure Determination. X-ray data for all three complexes were collected at 100 K at the Stanford Synchrotron Radiation Laboratory, beamline 7−1, equipped with a MAR imaging plate and processed using the program Denzo (Otwinowski, 1993; Minor, 1993). The crystals belong to space group $P2_1$, with one molecule per asymmetric unit (Table 1). To prepare the crystals for cryocooling, a mixture of 25% glycerol and 25% PEG 3350 was added to the crystal drop in 5 1 μL increments over 24

[2] In the following text, a segment of double-stranded DNA containing a 1 nt gap is abbreviated as "gap", and a segment of double-stranded DNA containing a nick is abbreviated as "nick". Both a gap and a nick are composed of a template strand, primer strand, and downstream oligo. In a gap, the loss of a nucleotide separates the primer and downstream oligo. In a nick, a broken phosphodiester linkage separates the 3′-OH of the primer and 5′-PO_4 of the downstream oligo.

Table 1: Data Collection and Refinement Statistics for Human DNA Polymerase β Structures

	data collection									refinement						
	unit cell									rms deviation		atoms modeled				
complex	*A*	*B*	*C*	β (deg)	d_{min} (Å)	I^o/σ	total observations/unique reflections	completeness (%)	R_{sym}[b]	bond (Å)	angle (deg)	protein	DNA	solvent	final[c] R	PDB code
gap	52.8	79.4	54.6	106.3	2.4	2.1	48472/165326	97	0.047	0.020	3.0	2653	633	83	0.253	1bpx
gap•ddCTP	50.5	79.8	54.9	107.1	2.2	5.5	54630/21036	95	0.086	0.021	3.0	2614	659	324	0.227	1bpy
nick	53.5	78.7	54.6	107.5	2.6	1.8	42489/14702	94	0.073	0.020	3.0	2653	651	27	0.243	1bpz

[a] Average ratio of observed intensity to σ in the highest resolution shell of reflections. [b] $R_{sym} = \sum|I_{obs} - I_{avg}|/\sum I_{avg}$. [c] Final $R = (\sum|F_{obs} - F_{calc}|/\sum F_{obs})$ including all data between 20 Å and d_{min}.

h. The Merlot molecular replacement package (Fitzgerald, 1988) was used to determine the initial set of phases for the ternary complex. The human pol β complex with blunt-ended DNA (PDB entry code 9icw) was used as a search model. When coordinates for the thumb subdomain were deleted from the model, the rotation and translation solutions were greater than 5σ and unambiguous. Later, it was found from examination of the electron density map that the thumb subdomain moved relative to the search model. The structure was then refined using the TNT least-squares refinement program (Tronrud et al., 1987). Initially rigid body refinement was employed, and then individual atomic positional and temperature factor refinement. Starting models for the two binary complexes were taken from the refined ternary complex in which coordinates for the thumb had been deleted. Rigid body refinement was employed, followed by individual atomic positional and temperature factor refinement. Examination of an $F_o - F_c$ difference Fourier map showed weak electron density for the thumb subdomain, but in a different conformation (open conformation) than in the ternary complex (closed conformation). Because the electron density of the thumb appeared about half as strong as the other subdomains of the polymerase, atoms of the thumb were given 0.5 occupancy. All structures refined with good geometry (rms deviation in bond lengths 0.020−0.021 Å, rms deviation in bond angles of 3.0°). Among the three structures, no backbone torsion angles lie in disallowed regions of the Ramachandran plot. At the worst, only three residues lie in generously allowed regions. *R*-factors range between 22.7% and 25.3% (Table 1).

Lowering the free *R*-factor has proven difficult. The simulated annealing algorithm of the X-PLOR refinement program has been suggested to aid in reaching the global minima of the *R*-factor function (Brünger, 1992). Simulated annealing was used in the refinement of the ternary complex. The output of this program was compared with the TNT refined model. Differences found in the X-PLOR refined model that provided a better fit to electron density were incorporated in the TNT refined model and then further refined with TNT. However, the free *R*-factor for the ternary complex did not fall below 32.5%. The average temperature factor for main chain atoms of the ternary complex is also rather high, approximately 40 Å^2. The high average temperature factor suggests that static disorder may explain the relatively high *R*-factors; the disorder may not be adequately modeled by isotropic temperature factors as employed.

RESULTS AND DISCUSSION

Geometry of Nucleotidyl Transfer at 2.2 Å Resolution. Previous structural studies of the rat pol β•template-primer•ddCTP ternary complex have offered several insights into the mechanism of nucleotidyl transfer (Pelletier et al., 1994). For instance, the in-line geometry of direct nucleophilic attack is apparent from the position of the primer's 3′ terminus and ddCTP's Pα and bridging phosphoryl oxygen. Also apparent from the rat pol β structure is the employment of two metal ions in the mechanism (a nucleotide-binding Mg^{2+} and a catalytic Mg^{2+}), a feature found in many phosphoryl transfer enzymes (Sträter et al., 1996). However, interpretations of more detailed structural aspects of catalysis, such as the geometry of Mg^{2+}•dNTP coordination, were limited by the resolution of the data, 2.9 Å. Some of these interpretations differ from the geometry found in the higher

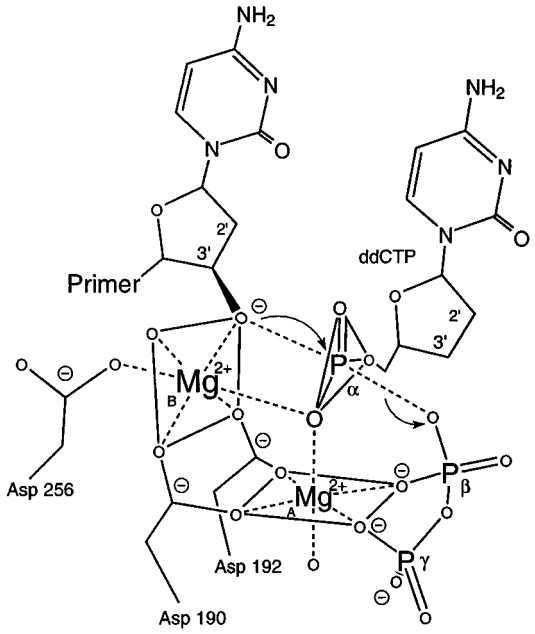

FIGURE 1: Schematic of proposed nucleotidyl transfer mechanism of pol β. The 3′-OH of the primer makes an in-line nucleophilic attack on Pα of ddCTP, the reactant present in the ternary complex crystals. The α-phosphate is coordinated by two metal ions, the nucleotide-binding ion (site A) and the catalytic ion (site B). ddCTP is coordinated as an α,β,γ-tridentate. The metal ions are anchored to the active site by coordinating the three conserved aspartates, Asp190, Asp192, and Asp256. Unexpectedly, no positive charge is in proximity of the forming oxyanion of the leaving pyrophosphate group. The water molecule (upper left) coordinated to the catalytic ion is not actually observed in the electron density map, but is hypothesized to complete the coordination sphere and channel the proton from the primer hydroxyl to solvent. The water molecule (bottom) coordinated to the nucleotide-binding ion is visible in the electron density map and is a newly observed structural feature.

resolution human pol β·gap·ddCTP ternary complex structure reported here. The differences are clearly due to the higher resolution of the human pol β ternary complex (2.2 Å vs 2.9 Å) rather than to the few amino acid sequence differences which are conservative and are located far from the active site (Pelletier et al., 1996a). Specifically, there are three noteworthy observations involving the metal ion coordination of ddCTP's triphosphate moiety. (1) The nucleotide-binding Mg^{2+} ion is now observed to coordinate the α-phosphate oxygen of ddCTP, completing the cation's octahedral coordination shell and modifying our previous description of a β,γ-bidentate (Pelletier et al., 1994) to an α,β,γ-tridentate (Figure 1). (2) The nonbridging α-phosphate oxygen now appears to be coordinated by both the nucleotide-binding Mg^{2+} and the catalytic Mg^{2+}, rather than just the latter ion (Figure 1). (3) No positively charged group is found in the vicinity of the forming oxygen anion of the pyrophosphate leaving group. This higher resolution view of the geometry of ion·dNTP coordination has implications for the mechanisms of nucleotidyl transfer proposed by Burgers and Eckstein (1979) and Joyce and Steitz (1995).

Burgers and Eckstein (1979) proposed that dNTP is coordinated as a β,γ-bidentate in the pol I active site and that the charge on the α-phosphate oxygen is neutralized by a positive group on the enzyme, rather than a metal ion. In their studies, metal ion coordination of α-phosphate was ruled out because stereoselectivity against the R_p dATPαS stereoisomer is retained when Mg^{2+} is replaced with a transition metal such as Co^{2+}, Mn^{2+}, or Zn^{2+}. Burgers and Eckstein argued that if stereoselectivity were lost, it would imply that the transition metal is able to coordinate the thio group (as transition metals are known to coordinate sulfur more readily than Mg^{2+}). But, since pol I cannot catalyze nucleotidyl transfer with the R_p stereoisomer, it was assumed that an enzyme group rather than a metal ion is involved as the charge neutralizing agent. The structure of human pol β·gap·ddCTP reveals, on the contrary, no positively charged enzyme group near the α-phosphate. Instead, there are two Mg^{2+} ions neutralizing the charge on the α-phosphate: the nucleotide-binding ion coordinates dNTP as an α,β,γ-tridentate, and the catalytic metal ion coordinates dNTP as an α-monodentate (Figure 1). If it is assumed that the nucleotidyl transfer mechanism utilized by pol I is similar to that in pol β, then these structural and kinetic results remain to be reconciled. In R_p dATPαS, it is the sulfur atom that is coordinated by two metal ions. Perhaps substituting two larger transition metal ions for two Mg^{2+} ions distorts the geometry of sulfur coordination, causing stereoselectivity against the R_p stereoisomer to be retained.

A more general mechanism for nucleotidyl transfer has been proposed based on analogy with 3′-5′ exonuclease and alkaline phosphatase complex structures as well as a host of other phosphoryl transfer enzymes (Joyce & Steitz, 1995; Steitz & Steitz, 1993). This mechanism involves two metal ions: one which coordinates the attacking anion, and a second which coordinates the leaving anion. Both metal ions also coordinate the nonbridging α-phosphate oxygen. Besides activating the attacking and leaving groups, this geometry is assumed to stabilize the pentacovalent transition state by inducing O−P−O bond angles near 90° between bridging and nonbridging phosphate oxygens. In the case of pol β, two features of the model seem to be true. The attacking 3′-OH appears activated by one of the metal ions, and both metal ions do coordinate the α-phosphate oxygen. However, the negative charge developing on the leaving group (the Pα−Pβ bridging oxygen) is not stabilized by coordination to either metal ion in the human pol β ternary complex structure. (Model building suggests that α,β,γ-tridentate coordination of the dNTP would not allow coordination of bridging oxygens, no matter how the triphosphate backbone were contorted.) In fact, there is no enzyme group in the vicinity available to stabilize negative charge formation on the bridging oxygen. Perhaps because the bond being broken is a phosphoanhydride rather than a phosphodiester bond (as is the case in nucleases), the bond is more labile to nucleophilic substitution. Spontaneous hydrolysis of tripolyphosphate (Van Wazer et al., 1955), though extremely slow at neutral pH and 25 °C, is 10^5 times faster than hydrolysis of a phosphodiester bond (Radzicka & Wolfenden, 1995). Alternatively, formation of a six-membered chelate ring upon coordination of the β-phosphate may be sufficient to activate the pyrophosphate group for departure (Ferrin et al., 1986).

α,β,γ-*Tridentate Coordination of dNTP*. The significance of α,β,γ-tridentate coordination of dNTP by Mg^{2+} is uncertain, but such binding may be unique to polymerase active sites. Thus far, tridentate coordination as seen in pol β is rare among crystal structures of enzyme complexes with other nucleoside triphosphates (such as ATP or GTP) deposited with the Protein Data Bank. With the exception of cyclin dependent kinase 2 (1hck) (De Bond et al., 1993), triphosphates appear to chelate metal ions as bidentate or

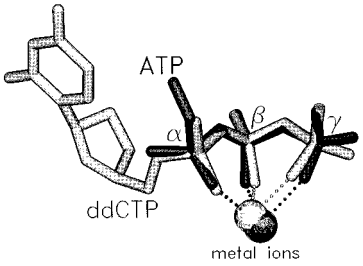

FIGURE 2: Conformation of triphosphate moiety. The structure of ddCTP from the ternary complex superimposes well with the triphosphate of Na^+·ATP, taken from the free molecule structure (Kennard et al., 1971; Sugawara et al., 1991). The Pα−Pβ distance in pol β and free dATP is about 4.1 Å. In most other enzyme complexes examined from the Protein Data Bank, the conformation of triphosphate (not shown) is extended with a Pα−Pβ distance of 5.1 ± 0.2 Å. The folded conformation of the triphosphate chain in pol β may be characteristic of all tridentate NTPs and dNTPs. This figure was produced using the graphics program Setor (Evans, 1993), as were Figures 3A and 5−8.

monodentate complexes. Enzymes examined include ras P21 (121p), elongation factor TU (1eft), GIα1 (1gia), transducin α (1tad), $tRNA^{Asp}$ synthetase (1asz), cAMP-dependent protein kinase (1cdk), biotin synthetase (1dag), $tRNA^{Glu}$ synthetase (1gtr), myosin head protein (1mmd), actin (1atn), heat shock protein (1nge), and phosphorylase kinase (1phk). Nevertheless, in solution an α,β,γ-tridentate Mg^{2+}·dNTP complex is in equilibrium with the β,γ-bidentate complex as suggested by ^{17}O NMR (Huang & Tsai, 1982), ^{31}P NMR (Bishop et al., 1981; Glonek, 1992), and several other solution studies of Mg^{2+}·ATP [see references in Wang et al., (1995)]. Furthermore, in crystals structures of free Na^+·ATP, the triphosphate is coordinated as a tridentate complex in a manner similar to that found in the pol β structure (Kennard et al., 1971; Sugawara et al., 1991) (Figure 2). The similarity in metal−phosphate coordination geometry between dNTP in solution and dNTP bound to enzyme may be a factor in accelerating the rate of dNTP binding and release. This feature may have special importance for polymerases since they must quickly discriminate between four dNTPs in solution for proper base pairing with the template.

Gapped DNA Substrate Binds with a 90° Kink. Most striking is the 90° kink in DNA observed in all three complexes reported here: gapped binary, gapped·ddCTP ternary, and nicked binary (Figure 3). The kink is located in the active site, precisely at the 5′-phosphodiester link of the template residue which base pairs with the incoming dNTP (i.e., the templating residue) (Figure 4). It is formed simply by rotating about the P−O5′ and the P−O3′ bonds by approximately 180° each from their normal B-DNA torsion angles. Both the upstream end of the gap/nick (11 nt) and the downstream end of the gap/nick (5 nt) correspond to B-DNA [as determined by use of the program Curves II (Lavery & Sklenar, 1989)], and their axes are crossed at 90°.

Each end of the gap is bound to a HhH motif, a motif found in many DNA repair enzymes (Thayer et al., 1995; Seeberg et al., 1995; Doherty et al., 1996; Pelletier et al., 1996a; Pelletier & Sawaya, 1996). The primer is bound to the HhH motif of the fingers subdomain with the same orientation and geometry as observed in the previously determined pol β−DNA complexes (Pelletier et al., 1994, 1996a; Pelletier & Sawaya, 1996). The downstream oligo of the gap/nick is bound to the HhH motif of the 8-kDa domain in a similar manner, as proposed earlier (Pelletier et al., 1996a) (Figure 4). The presence of multiple copies of the HhH motif in Ruv A suggests that Ruv A may accommodate the 90° kinks of a Holliday junction in a similar manner (Rafferty et al., 1996).

By binding the DNA with a 90° kink, pol β exposes the base pairs on either side of the kink, i.e., the base pair on the downstream side and the dNTP−template pair on the upstream side. The exposed base pair surface of the downstream side is stabilized by stacking interactions with the H34 imidazole ring and its backbone peptide plane (N-terminus of helix B, 8-kDa domain) (Figure 4). On the upstream side, the exposed base of the template residue stacks with the thumb's K280 peptide plane and side chain. The dNTP's base does not stack with the enzyme, but contacts the methylene group of Asp276. In the nicked DNA complex, the 5′-phospho group of the downstream oligo and the 3′-OH of the upstream primer (which would be consecutive nucleotide residues after the subsequent ligase reaction) are 25 Å apart.

The primary difference between the observed structure of the 1 nt gap complex (Figure 3) and the model of a 3 nt gap proposed by Pelletier et al. (1996a) (see Figure 9 therein) is in the position of the 8-kDa domain, which would seem to move with respect to the 31-kDa domain in response to gap size. The shorter the gap, the more contacts form between the 8-kDa domain and the 31-kDa domain. Specifically, in the 1 nt gapped DNA complex, helix A of the 8-kDa domain forms extensive contact with helices F and G of the fingers subdomain. Also unanticipated from the model, helix B of the 8-kDa domain forms extensive contacts with helix N of the thumb subdomain and the C-terminus (but only in the ternary complex when the thumb is closed, see below). Contact between the thumb subdomain and 8-kDa domain closes the open side of the U-shaped DNA-binding cleft into an O-shaped cleft. But the DNA is *not* threaded through the hole in the "O" as proposed for processivity factors (Krishna et al., 1994; Kong et al., 1992) (Figure 3C). Lastly, there is no indication of conversion of the Gly274−Ser275 *cis* peptide bond to the *trans* conformation as anticipated (Pelletier et al., 1996a).

Thumb Motion during the Catalytic Cycle. The catalytic cycle proceeds from gapped DNA binary complex to Michaelis ternary complex to nicked DNA binary complex. These are represented by the binary gapped DNA complex, the ternary complex with ddCTP, and the nicked DNA product. Structures of the gap and nick binary complexes, end points of the reaction coordinate, seem to differ only by the presence of a single nucleotide at the 3′ end of the primer strand; the additional nucleotide in the nicked binary complex simply fills the gap. But in the ternary complex, there is a closing rotation of the entire thumb subdomain (about a hinge axis approximately coincident with the axis of helix M), producing main chain movements up to 7 Å toward the active site (Figure 5). This hinge and its motion have been described in detail by Pelletier et al. (1996a). The data suggest that during the catalytic cycle, the thumb conformation proceeds from open to closed and back to the open conformation. Because all three complexes were crystallized in almost isomorphous packings (space group $P2_1$), the observed thumb motions ought to reflect ligand induced movements rather than crystal packing artifacts.

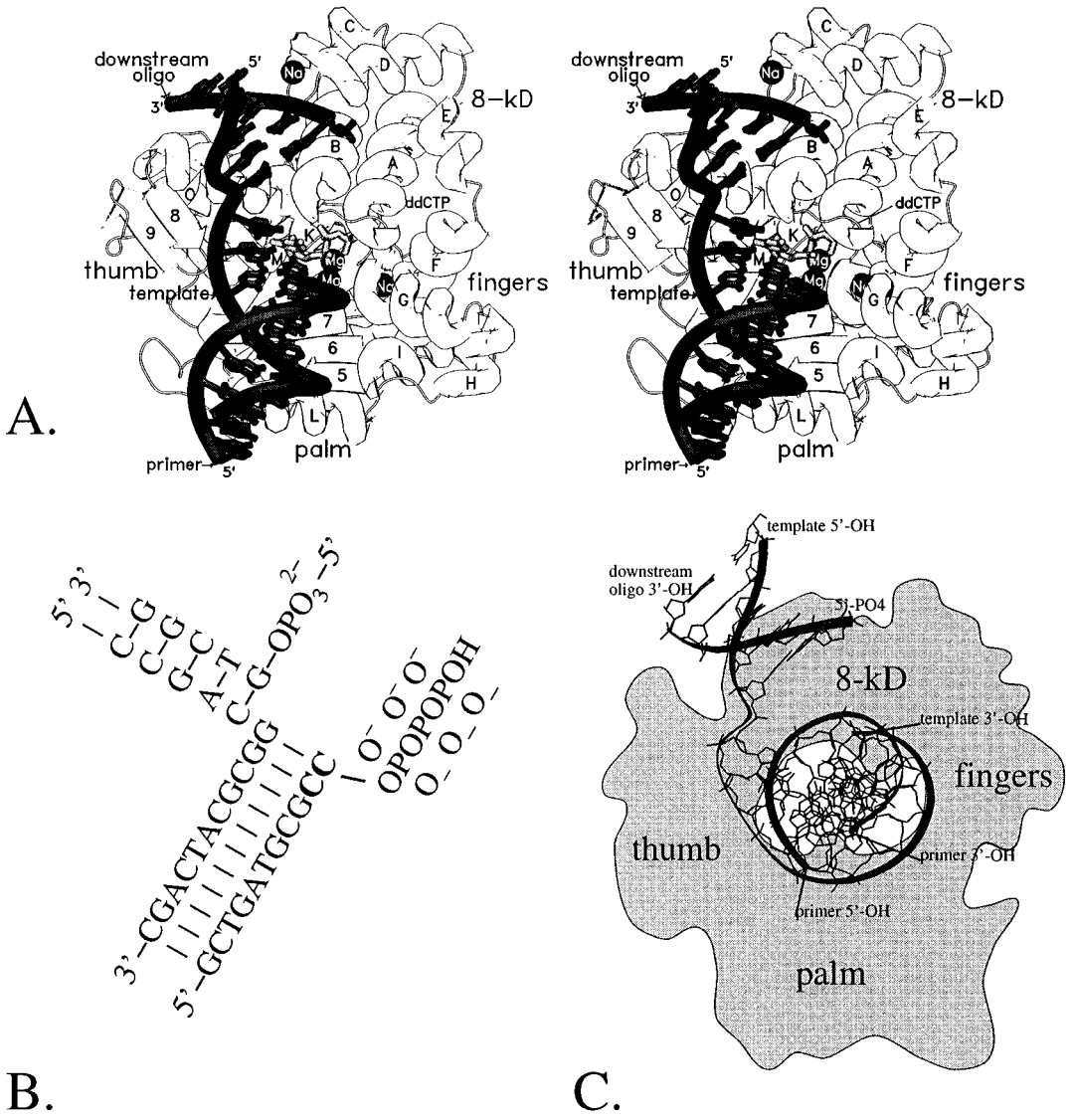

FIGURE 3: Crystal structure of the pol β·gap·ddCTP complex. Two magnesium ions and ddCTP mark the location of the active site. (A) Here, a sharp 90° kink in the templating residue separates the upstream and downstream portions of DNA. (B) Sequence of DNA used in crystallizing the pol β·gap·ddCTP complex. The two boldface C's derive from the added ddCTP. The 3′-terminal boldface C is shown as a triphosphate. The diagram is shown in the same orientation as the DNA in panel A. (C) The flexible 8-kDa domain (N-terminal) and thumb subdomain (C-terminal) contact each other, forming an "O" shaped cleft, but the DNA is not threaded through the "O" as might be expected. The view is slightly offset from the view in (A).

Active and Inactive Conformations of Pol β. Accompanying thumb movement is a host of small ($\approx$1−2 Å) and widely scattered conformational changes. The conformational changes seem to have their origin in movement of the thumb subdomain but are manifested directly at the site of nucleotidyl transfer: Asp192, dNTP, and template. These three elements of structure are found in either an active conformation or an inactive conformation as judged by their apparent ability to stabilize the transition state of nucleotidyl transfer. Thus, only the ternary complex, which displays a closed thumb, appears to be poised for catalysis of nucleotidyl transfer. In all other complexes which display an open thumb, these three elements of structure appear inactive. The same correlation between thumb conformation and the active site is observed in all seven crystal forms of pol β studied to date; the closed thumb/active form of the enzyme is found in rat (space groups $P2_1$ and $P6_1$) and human (space group $P2_1$) ternary complexes, and the open thumb/inactive forms are found in binary complexes and blunt-ended DNA ternary complexes (space group $P2_12_12$) (Pelletier et al., 1996a,b).

Asp192 is an active site residue within the conserved polymerase sequence motif C (Delarue et al., 1990; Sawaya et al., 1994). Conservative mutation of this residue to glutamic acid has been found to destroy nucleotidyl transfer activity in rat pol β (Date et al., 1991). However, though essential for catalysis, this residue is not always poised for catalysis throughout the catalytic cycle. Asp192 is found in either of two positions, differing by 120° rotation about χ_1. When the thumb is closed, Asp192 is coordinated by the nucleotide-binding metal ion, as expected for the nucleotidyl transfer step, while when the thumb is open, Asp192 is instead engaged in a salt bridge with Arg258. The closed thumb conformation favors the active Asp192 conformation in two ways. First, in the closed thumb conformation, the phenyl ring of Phe272 disrupts the salt bridge between Asp192 and Arg258, freeing Asp192 to ligand the nucleotide-binding metal ion (Figure 6). Second, and probably less important, the closed conformation puts the side chains of thumb residues Glu295 and Tyr296 in position to hydrogen

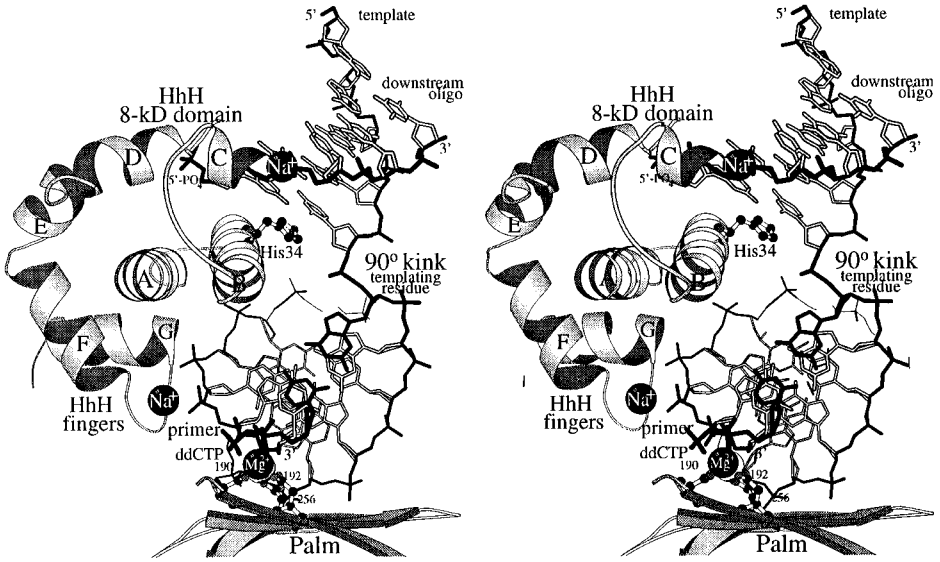

FIGURE 4: Close-up view of the 90° kinked template and its stabilizing interaction with two HhH motifs. The orientation of this view is similar to that of Figure 3A. ddCTP and its templating residue are drawn in bold black lines. Conserved aspartic acids are shown in a ball-and-stick representation. Most protein−DNA interactions are formed with the N-terminal 120 amino acids of pol β. Two HhH motifs, one in the 8-kDa domain and the other in the fingers subdomain, bind the downstream oligo and primer, respectively. The imidazole ring of His34 stacks with the downstream end of the gap. This figure was produced using the graphics program Molscript (Kraulis, 1991).

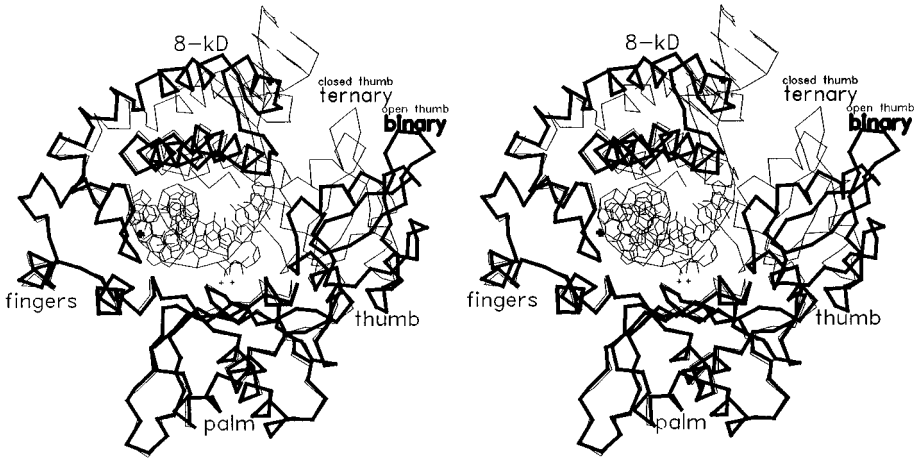

FIGURE 5: α-Carbon trace of pol β complexed with a 1 nt gap (thick lines) superimposed on the ternary complex with a 1 nt gap and ddCTP (thin lines). Most noticeable are the motions of the thumb (main chain movements up to 7 Å) and 8-kDa domain.

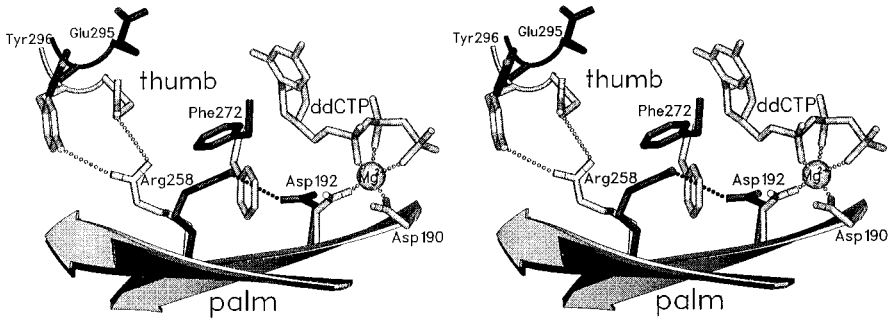

FIGURE 6: Response of catalytic Asp192 to the movement of the thumb subdomain. The ternary pol β·gap·ddCTP complex (gray) is superimposed on the binary pol β·gap complex (black) using α-carbons of the palm subdomain. Thumb closure activates the enzyme by moving Phe272 in position to disrupt the Arg258−Asp192 hydrogen bond, freeing Asp192 to bind both metal ions (only the nucleotide binding ion is shown). Thumb closure also moves thumb residues Glu295 and Tyr296 in position to engage Arg258 in hydrogen bonds, ensuring that Arg258 will not interfere with the Asp192 conformation.

bond with Arg258, ensuring that Arg258 will not interfere with Asp192's ability to ligand the metal ion (Figure 6). An Arg258→Ala mutation did not decrease k_{cat} (Menge et al., 1995), consistent with the idea that it removed a structural component of the inactive conformation.

In the nucleotidyl transfer reaction, the target of the primer's nucleophilic attack is Pα of the incoming dNTP. Yet, during the catalytic cycle, Pα may not always be properly positioned for attack by the primer. In fact, Pα is found in either of two positions, differing by approximately

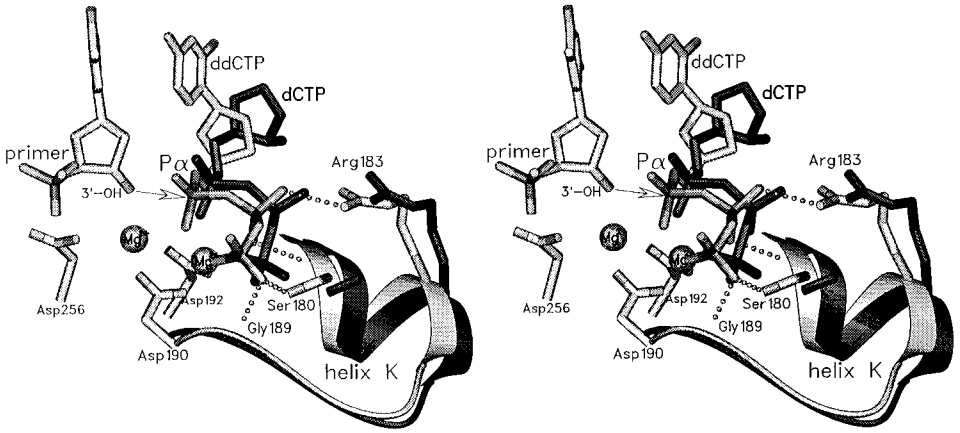

FIGURE 7: Response of the mononucleotide binding motif to movement of the thumb subdomain. The ternary pol β·gap·ddCTP complex (gray) is superimposed on the binary pol β·gap complex (black) using α-carbons of the palm subdomain. Thumb closure activates the enzyme by moving four hydrogen bond donors of helix K into position to interact with the β- and γ−phosphates of the incoming dNTP. Hydrogen bonds formed are Ser180(N)−dNTP(O2B), Ser180(Oγ)−dNTP(O2G), Arg183(NH2)−dNTP(O1B), and Gly189(N)−dNTP-(O2G). See Table 2 for hydrogen bond distances.

1 Å. When the thumb is closed (as in the ternary complex), Pα is 3.0 Å from the 3′-OH of the primer terminus,[3] close to the distance expected for nucleotidyl transfer. But when the thumb is open, as may be the case upon initial binding of dNTP, Pα is 1 Å further away from the primer. [The estimate of this latter distance is based on the distance between Pα and the 3′-OH of the primer in the previously reported human pol β complex with blunt-ended DNA and ddCTP (PDB entry code 8ict) where the thumb is open and there is no templating residue to base-pair with ddCTP (Pelletier et al., 1996a).] The thumb subdomain influences the position of Pα by shifting the entire mononucleotide binding motif (Sawaya et al., 1994) located in the palm subdomain (Figure 7). The motif is composed of helix K (residues 179−183) and the following loop (residues 184−189). Several thumb residues (Phe272, Thr273, Glu316, and Ser334) contact several helix K residues (Gly179, Arg182, Arg183), so that the thumb and mononucleotide-binding motif move essentially as a rigid body. When the thumb is closed, the mononucleotide-binding motif forms four strong hydrogen bonds with the dNTP's phosphate oxygens (Table 2; Figure 7). When the thumb is open, the mononucleotide-binding motif rotates away from the active site, drawing Pα away from the primer and weakening interactions with the dNTP's phosphates as evidenced by 0.5−1.0 Å longer hydrogen bond lengths. Thumb closure favors the active dNTP conformation by moving the mononucleotide-binding motif closer to the primer 3′-OH.

The templating residue determines which dNTP reacts at the active site. However, during the catalytic cycle, the templating residue is not always properly positioned to base-pair with dNTP. Depending on the thumb conformation, the templating residue and the following two nucleotide residues exist in active or inactive states, differing by 20 Å^2 in average temperature factor and 1 Å in position. When the thumb is closed as in the ternary complex, these residues are well ordered. But, when the thumb is open, as in the binary gapped and nicked complexes, these template residues become more disordered. The 20 Å^2 difference represents the largest difference in temperature factor between the DNA molecules in the binary and ternary complexes. Consequently, these three template residues display the highest temperature factors among all DNA residues. Furthermore, the phosphodiester backbone is translated 1 Å away from the thumb (Figure 8). Thumb closure favors the active template conformation by directly forming van der Waals contacts with the template, anchoring it to the polymerase. [In a similar way, thumb closure may anchor the primer by forming a hydrogen bond between thumb residue Tyr271-(OH) and the primer base CytP10(O2) (Table 2).]

Table 2: Comparison of Thumb−Nucleic Acid Contacts in Binary and Ternary Pol β Complexes

nucleic acid		thumb		distances (Å)		
residue	atom	residue	atom	binary gap	ternary gap	binary nick
ddCTP	C4	Asp276	Cβ	−	3.5	−
	O1B	Arg183	NH2	3.8[a]	2.9	−
	O2B	Ser180	N	3.4[a]	2.8	−
	O2G	Ser180	Oγ	2.9[a]	2.3	−
	O2G	Gly189	N	3.4[a]	2.5	−
primer	P10 O2	Tyr271	OH	6.9	2.5	6.2
template	T6 N3	Arg283	Cδ	10.1	3.6	9.0
	T7 O2P	Thr292	Oγ1	10.3	3.0	10.2
	T7 O4′	Arg283	NH1	8.2	2.6	7.1
	T8 O3′	Glu295	Oϵ2	7.3	3.3	6.5
	T9 O2P	Tyr296	OH	5.3	2.9	4.5

[a] Distances taken from human pol β complex with blunt-ended DNA and dCTP (PDB entry 8ict) (Pelletier et al., 1996b). dCTP binding geometry in this complex may represent the initial binding of dNTP to binary gap complex, in which the thumb is in the open conformation.

Thumb Movement in Translocation and Fidelity. When filling a gap less than or equal to 6 nt, pol β has been shown to translocate along the template-primer to fill in the next nucleotide (Singhal & Wilson, 1993; Prasad et al., 1994). Thumb movement may be involved in this translocation step. In both binary gap and binary nick complexes, the thumb appears to be open. The loss of contacts between thumb and template following nucleotidyl transfer probably facilitates translocation of pol β along the template-primer. When the gap is filled, as observed in the nicked DNA complex, the thumb opens again to allow the product to dissociate.

[3] The position of the 3′-OH is modeled based on coordinates of C3′. Recall that in the ternary complex the primer is terminated by a 2′,3′-dideoxynucleotide.

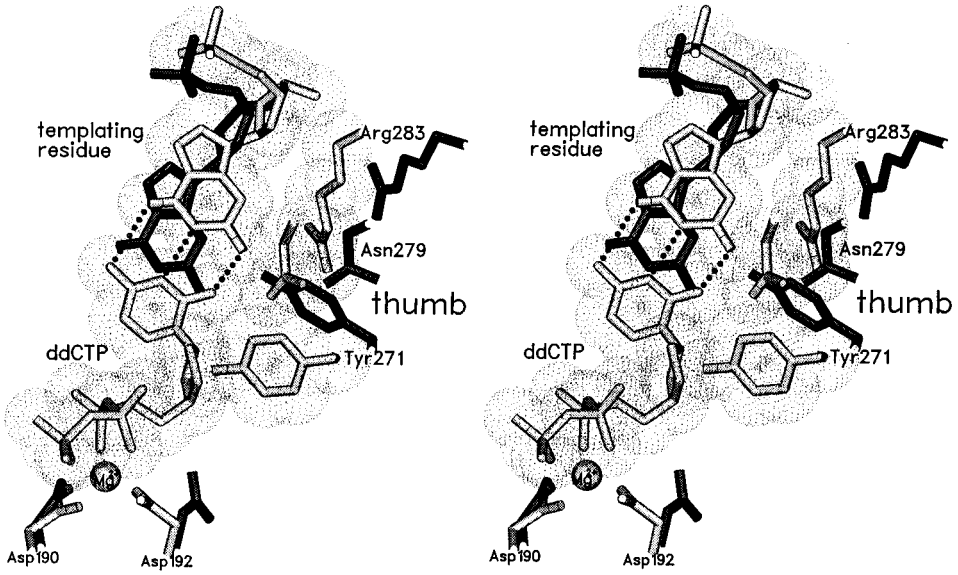

FIGURE 8: Response of template residues to movement of the thumb subdomain. The ternary pol β·gap·ddCTP complex (gray) is superimposed on the binary pol β·gap complex (black) using α-carbons of the palm subdomain. The orientation of this view is similar to that of Figure 3C. Template residue T6 is the residue which base-pairs with incoming dNTP. Thumb closure lowers the temperature factors (by 20 Å^2 of this and two adjacent residues. The DNA sugar−phosphate backbones in the two complexes also differ in position by approximately 1.0 Å.

Another intriguing possibility is that thumb movement plays a role in enhancing fidelity via an induced fit mechanism (Koshland, 1958, 1994). To demonstrate the existence of an induced fit mechanism requires the observation of three criteria. (1) There are two conformations of the active site, active or inactive, depending on whether the thumb is closed or open, respectively. (2) The conformational change is triggered by specific base-pairing of substrate dNTP to a templating residue, assembling the active site. (3) The conformational change is *not* triggered by the incorrect dNTP.

Evidence for criterion (1), the existence of active and inactive conformations of the polymerase, was detailed in the previous section. In summary, until the thumb closes, the active site is incompletely assembled: Asp192 will favor a conformation which cannot ligand the nucleotide-binding metal ion, Pα of the incoming dNTP will be over 1 Å further from the primer's 3′-OH, and the templating residue will be disordered. These observed structural perturbations may correspond to the partially rate-limiting conformational change observed in pol β kinetics (Werneberg, 1996). As noted by Pelletier et al. (1996a), a rate-limiting conformational change is characteristic of several other well-studied polymerases.

In support of criterion (2), it is also clear that dNTP binding *and* base-pairing with the template correlate with thumb closure. Out of seven crystal forms observed, the thumb is closed only in the three ternary complexes in which a ddNTP base-pairs with the template. dNTP binding in the absence of a templating residue is not sufficient to effect thumb closure, as observed in previously determined human pol β complexes with blunt-ended template-primer and dNTP (e.g., PDB entry 8ict) (Pelletier et al., 1996b). Furthermore, the triphosphate moiety of dNTP also appears essential for thumb closure since the thumb remains open in the nicked DNA complex, despite proper base-pairing in the active site. Interactions between the triphosphate moiety and mononucleotide-binding motif anchor dNTP to the palm. When dNTP base-pairs with the template, it is reasonable to assume that the template becomes anchored also. Once the template is anchored, thumb closure may be stabilized by contact between the thumb and template (Table 2; Figure 8).

Criterion (3), selectivity of the conformational change for the correct dNTP, remains to be established. Perhaps irregularities in nucleotide geometry or the inclusion of water molecules in mismatched base pairs may be detected by contact with thumb residues, thus inhibiting thumb closure and preventing proper assembly of the active site. Crystallographic studies of A·C and T·G mismatches in DNA reveal asymmetrical dispositions of the glycosyl bonds with respect to the vector between ribose C1′−C1′ atoms, producing 0.5 Å shorter C1′−C1′ distances (Hunter et al., 1986). Such significant distortions exist despite the fact that these two mismatches best mimic the base pair geometry of normal Watson−Crick pairs. Other mismatches involve still more distorted geometry, such as the *syn* N-glycosidic conformation or perturbations in the rise per base pair (up to 0.4 Å) (Hunter et al., 1987; Brown, 1995). Also, water molecules are often found as a structural component of mismatch geometry (Hunter et al., 1987). Arg283 in particular, which contacts the minor groove edge of the templating residue, has been identified in mutagenesis studies to be required for nucleotide discrimination; mutation to alanine causes a 160-fold decrease in fidelity (Beard et al., 1996) (Figure 8). (No other mutation currently studied has such a deleterious effect on fidelity.) Perhaps if the base pair is incorrect, the enthalpy of interaction between template and thumb is insufficient to close the thumb and assemble the active site. Or perhaps the presence of Arg283 excludes water from the minor groove, destabilizing the mismatch base pair and enhancing fidelity (Petruska et al., 1988). Crystallographic evidence indicates that the thumb does indeed remain open when a A-ddGTP mismatch occurs in the polymerase active site (Sawaya and Kraut, unpublished results).

Whether conformational changes can, in theory, actually enhance specificity via an induced fit mechanism has been a controversial question for many years. Answers vary, depending on which kinetic step is rate-limiting: substrate

binding, the chemical step, or product release (Herschlag, 1988). In a more general formulation, Post and Ray (1995) suggest that induced fit can enhance fidelity if a chemically important conformational distinction is allowed to persist in the transition state containing correct versus incorrect substrate. Such a distinction can easily be visualized in the active site of pol β. In the case of correct dNTP-template pairing, the thumb favors the closed conformation, triggering numerous other movements which stabilize the transition state of nucleotidyl transfer; Asp192 is poised for catalysis, Pα of the dNTP is positioned for nucleophilic attack, and the template is ordered. In the case of incorrect dNTP pairing, the thumb may remain open or disordered, resulting in a transition state in which Asp192, dNTP, and the template are in unfavorable conformations for nucleotidyl transfer. Isotope effects are consistent with the distinction between transition states; chemistry is indeed rate limiting for the incorrect dNTP but only partially rate-limiting for the correct dNTP (Werneberg et al., 1996).

Assuming that the proposed induced fit mechanism does indeed enhance fidelity in pol β, what is the magnitude of this enhancement? Pol β is one of the most error-prone polymerases known. According to a reversion fidelity assay using a 5 nt gap DNA substrate, pol β's error frequency is 1 in 2000 nucleotides if the T·dGTP mismatch is excluded from calculations. If this anomalously frequent mismatch is included, the error rate jumps to 1 in 670 nucleotides (Beard et al., 1996). Estimates of the error rate that would arise from free energy differences between correct and incorrect pairing in solution range from 1 in 10 to 1 in 300 (Raszka & Kaplan, 1972; Mildvan, 1974; Lohrmann & Orgel, 1980). Therefore, the fidelity enhancement factor provided by pol β appears to lie somewhere between 2- and 200-fold, leaving open to question the role of the proposed induced fit mechanism. It is possible that the observed thumb movements evolved solely for the purpose of facilitating translocation. However, the unmistakable correlation of thumb motion with assembly and disassembly of the active site argues strongly that these movements do indeed enhance fidelity via an induced fit mechanism.

Role of 90° Kinked DNA. It is interesting to speculate on why DNA should be kinked in this fashion when bound to pol β. In the base excision repair pathway, after the AP site is removed, a single-stranded gap is formed. There are no strong torsional constraints on single-stranded DNA, so kinking to some degree is an inevitable and probably an identifying feature of pol β's gap substrate. Pol β's ability to recognize this feature may facilitate recognition of damaged DNA.

The 90° kink and exposure of the base pairs on either end of the gap may also enhance fidelity in filling small gaps to completion. If the enzyme's substrate were linear, instead of kinked and exposed, the enzyme molecule would have little access to the base pair being formed, particularly when the gap is two nucleotides or less. However, when the gap is kinked, the template-dNTP base pair is exposed to the enzyme, increasing the surface area over which the enzyme may test for base pair correctness. If this hypothesis is correct, then a 90° kink at the 5′ side of the templating residue may be a salient feature of all polymerases involved in filling small gaps *to completion* as is pol β.

DNA Polymerase β Movies. Four movies have been constructed depicting thumb movement and the assembly/disassembly of the active site of pol β. The main purpose of the movies is to aid in comprehension of polymerase dynamics. These movies are based on the three human pol β structures reported here: the binary gap complex, the ternary gap·ddCTP complex, and the binary nick complex. The movies animate the conformational changes presented in Figures 5−8, showing the thumb close as ddCTP binds the binary gap complex, and then open again as the product nick complex is formed. Intervening frames of the movie were generated by interpolating coordinates between pairs of crystal structures. The movies are available on the Internet and may be viewed with the Netscape web browser at http://www-chem.ucsd.edu/Faculty/Kraut/bpol.html.

ACKNOWLEDGMENT

We thank the staff of the Stanford Synchrotron Radiation Laboratory for a grant of data collection time and for their expert assistance, especially M. Soltis, M. St. Pierre, J. Hadler, and S. Belopolskiy. We thank T. Kunkel for helpful discussions. We thank S. Everse and S. Ye for technical assistance. We acknowledge the San Diego Supercomputer Center for a grant of computing time.

REFERENCES

Abbotts, J., SenGupta, D. N., Zmudzka, B., Widen, S. G., Notario, V., & Wilson, S. H. (1988) *Biochemistry 27*, 901−909.
Beard, W. A., Osheroff, W. P., Prasad, R., Sawaya, M. R., Jaju, M., Wood, T. G., Kraut, J., Kunkel, T. A., & Wilson, S. H. (1996) *J. Biol. Chem. 271*, 12141−12144.
Beckman, R. A., & Loeb, L. A. (1993) *Q. Rev. Biophys. 26*, 225−331.
Bishop, E. O., Kimber, S. J., Orchard, D., & Smith, B. E. (1981) *Biochim. Biophys. Acta 635*, 63−72.
Brown, T. (1995) *Aldrichimica Acta 28*, 15−20.
Brünger, A. T. (1992) X-PLOR Version 3.1. *A System for X-ray Crystallography and NMR*, Yale University Press, New Haven and London.
Burgers, P. M. J., & Eckstein, F. (1979) *J. Biol. Chem 254*, 6889−6893.
Date, T., Yamamoto, S., Tanihara, K., Nishimoto, Y., & Matsukage, A. (1991) *Biochemistry 30*, 5286−5292.
Davies, J. F., Almassy, R. J., Hostomska, Z., Ferre, R., & Hostomsky, Z. (1994) *Cell 76*, 1123−1133.
De Bond, H. L., Rosenblatt, J., Jancarik, J., Jones, H. D., Morgan, D. O., & Kim, S.-H. (1993) *Nature 363*, 595−602.
Delarue, M., Poch, O., Tordo, N., Moras, D., & Argos, P. (1990) *Protein Eng. 3*, 461−467.
Doherty, A. J., Serpell, L. C., & Ponting, C. P. (1996) *Nucleic Acids Res. 24*, 2488−2497.
Echols, H., & Goodman, M. F. (1991) *Annu. Rev. Biochem. 60*, 477−511.
Ferrin, L. J., Beckman, R. A., Loeb, L. A., & Mildvan, A. S. (1986) in *Manganese in Metabolism and Enzyme Function* (Schramm, V. L., & Wedler, F. C., Eds.) pp 259−273, Academic Press, New York.
Fitzgerald, P. M. D. (1988) *J. Appl. Crystallogr. 21*, 273−278.
Freese, E. B., & Freese, E. (1967) *Proc. Natl. Acad. Sci. U.S.A. 57*, 650−657.
Glonek, T. (1992) *Int. J. Biochem. 24*, 1533−1559.
Herschlag, D. (1988) *Bioorg. Chem. 16*, 62−96.
Huang, S. L., & Tsai, M.-D. (1982) *Biochemistry 21*, 951−959.
Hunter, W. N., Brown, T., Anand, N. N., & Kennard, O. (1986) *Nature 320*, 552−555.
Hunter, W. N., Brown, T., Kneale, G., Anand, N. N., Rabinovich, D., & Kennard, O. (1987) *J. Biol. Chem. 262*, 9962−9970.
Johnson, K. A. (1993) *Annu. Rev. Biochem. 62*, 685−713.
Joyce, C. M., & Steitz, T. A. (1995) *J. Bacteriol. 177*, 6321−6329.
Kennard, O., Isaacs, N. W., Motherwell, W. D. S., Coppola, J. C., Wampler, D. L., Larson, A. C., & Watson, D. G. (1971) *Proc. R. Soc. London, Ser. A 325*, 401−436.

Kong, X. P., Onrust, R., O'Donnell, M., & Kuriyan, J. (1992) *Cell 69*, 425−437.
Kornberg, A. (1969) *Science 163*, 1410−1418.
Koshland, D. E. (1958) *Proc. Natl. Acad. Sci. U.S.A. 44*, 98.
Koshland, D. E. (1994) *Angew Chem., Int. Ed. Engl. 33*, 2375−2378.
Krishna, T. S., Kong, X. P., Gary, S., Burgers, P. M., & Kuriyan, J. (1994) *Cell 79*, 1233−1243.
Kumar, A., Abbots, J., Karawya, E. M., & Wilson, S. H. (1990) *Biochemistry 29*, 7156−7159.
Lavery, R., & Sklenar, H. (1989) *J. Biomol. Struct. Dyn. 6*, 655.
Lindahl, T. (1993) *Nature 362*, 709−715.
Lohrmann, R., & Orgel, L. E. (1980) *J. Mol. Biol. 142*, 555−567.
Matsumoto, Y., & Kim, K. (1995) *Science 269*, 699−702.
Menge, K. L., Hostomsky, Z., Nodes, B. R., Hudson, G. O., Rahmati, S., Moomaw, E. W., Almassy, R. J., & Hostomska, Z. (1995) *Biochemistry 34*, 15934−15942.
Mildvan, A. S. (1974) *Annu. Rev. Biochem. 43*, 357−399.
Minor, W. (1993) "XDISPLAYF Program", Purdue University.
Otwinowski, Z. (1993) *Proceedings of the CCP4 Study Weekend 29−30 January*, Compiled by: Sawyer, L., Isaacs, N., & Bailey, S., SERC Daresbury Laboratory, England, pp 56−62.
Pelletier, H., & Sawaya, M. R. (1996) *Biochemistry 35*, 12778−12787.
Pelletier, H., Sawaya, M. R., Kumar, A., Wilson, S. H., & Kraut, J. (1994) *Science 264*, 1891−1903.
Pelletier, H., Sawaya, M. R., Wolfle, W., Wilson, S. H., & Kraut, J. (1996a) *Biochemistry 35*, 12742−12761.
Pelletier, H., Sawaya, M. R., Wolfle, W., Wilson, S. H., & Kraut, J. (1996b) *Biochemistry 35*, 12762−12777.
Petruska, J., Goodman, M. F., Boosalis, M. S., Sowers, L. C., Cheong, C., & Tinoco, I., Jr. (1988) *Proc. Natl. Acad. Sci. U.S.A. 85*, 6252−6256.
Post, C. B., & Ray, W. J., Jr. (1995) *Biochemistry 34*, 15881−15885.
Prasad, R., Beard, W. A., & Wilson, S. H. (1994) *J. Biol. Chem. 269*, 18096−18101.
Radzicka, A., & Wolfenden, R. (1995) *Science 267*, 90−93.
Rafferty, J. B., Sedelnikova, S. E., Hargreaves, D., Artymiuk, P. J., Baker, P. J., Sharples, G. J., Mahdi, A. A., Lloyd, R. G., & Rice, D. W. (1996) *Science 274*, 415−421.
Raszka, M., & Kaplan, N. O. (1972) *Proc. Natl. Acad. Sci. U.S.A. 69*, 2025−2029.
Sawaya, M. R., Pelletier, H., Kumar, A., Wilson, S. H., & Kraut, J. (1994) *Science 264*, 1930−1935.
Seeberg, E., Eide, L., & Bjoras, M. (1995) *Trends Biochem. Sci. 20*, 391−397.
Singhal, R. K., & Wilson, S. H. (1993) *J. Biol. Chem. 268*, 15906−15911.
Sobol, R. W., Horton, J. K., Kühn, R., Gu, H., Singhal, R. K., Prasad, R., Rajewsky, K., & Wilson, S. H. (1996) *Nature 379*, 183−186.
Steitz, T. A., & Steitz, J. A. (1993) *Proc. Natl. Acad. Sci. U.S.A. 90*, 6498−6502.
Sträter, N., Lipscomb, W. N., Kabunde, T., & Krebs, B. (1996) *Angew. Chem., Int. Ed. Engl. 35*, 2024−2055.
Sugawara, Y., Kamiya, N., Iwasaki, H., Ito, T., & Satow, Y. (1991) *J. Am. Chem. Soc. 113*, 5440.
Thayer, M. M., Ahern, H., Xing, D., Cunningham, R. P., & Tainer, J. A. (1995) *EMBO J. 14*, 4108−4120.
Tronrud, D. E., Ten Eyck, L. F., & Matthews, B. W. (1987) *Acta Crystallogr. A43*, 489−501.
Van Wazer, J. R., Griffith, E. J., & McCullough, J. F. (1955) *J. Am. Chem. Soc. 77*, 287−291.
Wang, P., Oscarson, J. L., Izatt, R. M., Watt, G. D., & Larsen, C. D. (1995) *J. Solution Chem. 24*, 989−1012.
Werneberg, B. G., Ahn, J., Zhong, X., Hondal, R. J., Kraynov, V. S., & Tsai, M.-D. (1996) *Biochemistry 35*, 7041−7050.
Wong, I., Patel, S. S., & Johnson, K. A. (1991) *Biochemistry 30*, 526−537.

BI9703812